

# Recycling and Imaging of Nuclear Singlet Hyperpolarization

Giuseppe Pileio<sup>1,\*</sup>, Sean Bowen<sup>2</sup>, Christoffer Laustsen<sup>3,4</sup>, Micheal C. D. Tayler<sup>1,†</sup>, Joseph T. Hill-Cousins<sup>1</sup>, Lynda J. Brown<sup>1</sup>, Richard C. D. Brown<sup>1</sup>, Jan H. Ardenkjaer-Larsen<sup>2,4,5</sup> and Malcolm H. Levitt<sup>1</sup>

<sup>1</sup> Department of Chemistry, University of Southampton, Southampton, SO17 1BJ, UK; <sup>2</sup> Technical University of Denmark, Department of Electrical Engineering, Lyngby, DK. <sup>3</sup> The MR Research Centre, Aarhus University Hospital, Aarhus, DK. <sup>4</sup> Danish Research Centre for Magnetic Resonance, Hvidovre Hospital, Hvidovre, DK. <sup>5</sup> GE Healthcare, Park Alle 295, 2605 Broendby, DK.

---

**ABSTRACT:** The strong enhancement of NMR signals achieved by hyperpolarization, decays, at best, with a time constant of a few minutes. Here we show that a combination of long-lived singlet states, molecular design, magnetic field cycling, and specific radiofrequency pulse sequences, allows repeated observation of the same batch of polarized nuclei over a period of 30 minutes and more. We report a recycling protocol in which the enhanced nuclear polarization achieved by dissolution-DNP is observed with full intensity and then returned to singlet order. E.g. MRI experiments may be run on a portion of the available spin polarization while the remaining is preserved and made available for a later use. An analogy is drawn with a "spin bank" or "resealable container" in which highly polarized spin order may be deposited and retrieved.

---

## 1. Introduction

Nuclear polarization enhancement techniques can boost NMR signals of room temperature liquid samples more than 4 orders of magnitude above those from thermal equilibrium polarization. The combination of low-temperature dynamic nuclear polarization (DNP<sup>1-3</sup>) with fast sample dissolution (dissolution-DNP<sup>4,5</sup>), for example, routinely produces liquid-state NMR signals whose signal-to-noise has been enhanced by 10,000 times. However, this extraordinary enhancement is often under-exploited due to the short lifetime of the nuclear spin magnetization. Strongly polarized nuclear spin magnetization decays with a time constant,  $T_1$ , which typically spans the range from a few milliseconds up to a few minutes.

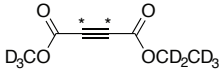
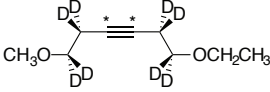
The lifetime of nuclear spin order in spin-1/2 pairs may be extended beyond  $T_1$  by exploiting nuclear singlet states<sup>6,7</sup>. These states are immune to the pair symmetric component of spin relaxation mechanisms, the most notable of which is the intra-pair dipole-dipole mechanism, which is completely symmetric<sup>8</sup>. In cases where such mechanisms dominate the nuclear spin relaxation, the lifetime of nuclear singlet order, denoted  $T_S$ , may exceed  $T_1$ , often with dramatic effect. Moreover, singlet order is often less sensitive than longitudinal order to relaxation mechanisms other than dipolar, if some conditions are met<sup>8-12</sup>. The singlet lifetime of <sup>15</sup>N nitrous oxide (<sup>15</sup>N<sub>2</sub>O) is for instance almost half-an-hour in organic solvents<sup>13</sup> ( $T_S \sim 8 T_1$ ), and 7 minutes in human blood<sup>14</sup>. Singlet lifetimes exceeding 10 minutes, or in excess of 20  $T_1$ , have been measured for <sup>13</sup>C spin pairs in organic molecules at both high and low magnetic fields<sup>15</sup>. Franzoni and co-workers recently reported on the vinyl <sup>1</sup>H pair in dimethyl maleate, which exhibits a staggering four-minute singlet lifetime<sup>16</sup>.

Several demonstration of using long-lived singlet states for storage of enhanced polarization have already been made<sup>17-20</sup>. However, so far, all of these demonstrations employed one of two procedures, both of which suffer major disadvantages:

*One-shot observation.* The enhanced singlet polarization is completely converted into transverse magnetization, generating a strong NMR signal. This method has the advantage that the full magnitude of the spin order is exploited. However, the polarization is destroyed completely by the observation process. No further NMR experiments can be conducted, without regenerating the polarization.

*Perturbative observation.* A small amount of singlet order is converted into transverse magnetization, which is then observed<sup>17-20</sup>. In this case, most of the polarization remains in the form of singlet order, which may be converted to

magnetization and observed at a later time. In this respect the method resembles the use of small flip-angle pulses to monitor hyperpolarized longitudinal magnetization<sup>21-23</sup>. The disadvantage of this scheme is that only a small fraction of the polarized spin order is observed at any one time, leading to much weaker signal strength.

Sample	Solvent	Structure	Field	T <sub>1</sub>	T <sub>S</sub>
1	CD <sub>3</sub> CN		2.2mT	44s	800s
2	CD <sub>3</sub> OD		9.4T	27s	577s

**Figure 1.** Molecular structure and relaxation parameters for the two samples used in the experiments. The asterisks denote <sup>13</sup>C labels.

In this paper we propose an alternative approach in which the same batch of highly polarized nuclei is observed with full intensity and its polarization reconverted to long-lived singlet order with only a small intensity loss. Multiple observations of spin magnetization over a total time of half-an-hour are reported.

In a variant of the method, we demonstrate how two portions of highly polarized nuclei are separately stored in the high field of a MRI scanner and accessed, independently, to collect two different series of NMR images.

## 2. Methods

### 2.1 Samples

Two <sup>13</sup>C<sub>2</sub>-labelled samples, whose relaxation properties have been previously investigated<sup>15</sup>, were used for the demonstration experiments. The molecular structures and relaxation properties are summarized in Figure 1.

*Sample 1.* 1-Ethyl-4-methyl but-2-ynedioate-2,3-<sup>13</sup>C<sub>2</sub>,d<sub>8</sub> (Fig. 1, sample 1) was synthesized as described in the Supporting Information. Sample 1 dissolved in acetonitrile-d<sub>3</sub>, and degassed to remove molecular oxygen has a singlet order decay time constant T<sub>S</sub> ~800 s (nearly 20 T<sub>1</sub>) in low magnetic field<sup>15</sup> (~2 mT). The difference in isotropic chemical shift is ~0.62 ppm (~62 Hz in a 9.4 T magnet) and the <sup>13</sup>C-<sup>13</sup>C J-coupling is 185 Hz. The relatively large isotropic shift difference leads to rapid singlet-triplet transitions in high magnetic field, so the singlet order only displays its long-lived nature when the sample is transported to a region of low magnetic field (of the order of about 2 T or less).

*Sample 2.* 1-Ethoxy-6-methoxyhex-3-yne-3,4-<sup>13</sup>C<sub>2</sub>-1,1,2,2,5,5,6,6-d<sub>8</sub> (Fig. 1, sample 2) was synthesized as described in the Supporting Information. The difference in isotropic chemical shift is ~0.13 ppm (~6.5 Hz in a 4.7 T magnet) and the <sup>13</sup>C-<sup>13</sup>C J-coupling is 180 Hz. Since the isotropic chemical shift difference is small, singlet-triplet transitions are well suppressed without intervention, even in relatively high magnetic field. Sample 2 dissolved in deuteromethanol, and degassed to remove molecular oxygen has a singlet order decay time constant T<sub>S</sub> ~600 s (nearly 20 T<sub>1</sub>) at a field of 7 T and below<sup>15</sup>.

### 2.2 Hyperpolarization

Samples for hyperpolarization consisted of 15 mM AH111501 (Tris(8-carboxy-2,2,6,6 (tetra(methoxyethyl) benzo-[1,2-4,5□]bis-(1,3)dithiole-4-yl)methyl sodium salt) in 25% DMSO-d<sub>6</sub>, 25% methanol-d<sub>4</sub> and 50% of <sup>13</sup>C<sub>2</sub>-labelled Sample 1 or 2. The sample size was 2 μL for spectroscopy experiments and 20 μL for imaging experiments. The mixture was cooled to ~1.4 K in a magnetic field of 3.35 T and irradiated with 100 mW of microwave power at a frequency of ~94 GHz for about 1 hour. Once the signal enhancement reaches saturation (as observed by monitoring the solid-state NMR spectrum of the sample), the sample was rapidly dissolved by a hot solvent (CD<sub>3</sub>CN for spectroscopy and CD<sub>3</sub>OD for imaging experiments) and transported out of the polarizer. The polarized solution was transported into a high-resolution NMR spectrometer or an MRI scanner. The typical transport time was ~5 seconds with the sample never experiencing fields lower than the earth magnetic field. Although the dissolution-DNP procedure induces a small amount of highly polarized singlet order<sup>24</sup> along with magnetization, this contribution was ignored for the sake of simplicity.

## 3. Results

### 3.1 Recycled observation of highly polarized singlet order

Repeated observation of spin polarization was performed by combining M2S (magnetization-to-singlet) and S2M (singlet-to-magnetization) pulse sequences<sup>25-27</sup> with a triplet-echo (TE) pulse sequence, as shown in Figure 2. The triplet-echo consists of the 5-pulse sequence 90<sub>90</sub>-τ/4-180<sub>0</sub>-τ/4-90<sub>0</sub>-τ/4-180<sub>0</sub>-τ/4-90<sub>90</sub> where the subscripts denote pulse phases,

and the total echo duration is  $\tau$ . The two outer pulses convert the longitudinal magnetization generated by the S2M pulse sequence to transverse magnetization, and return the transverse magnetization to longitudinal magnetization at the end of the sequence. The  $180^\circ$  pulses refocus chemical shifts and magnetic field inhomogeneities, while the central  $90^\circ$  pulse induces coherence transfer between the two single-quantum triplet-triplet coherences, thereby refocusing interactions which break the degeneracy of these two transitions. Similar refocusing is widely used in the spectroscopy of spin-1 nuclei (e.g. deuterium) in the solid state, where it forms the basis of the quadrupolar echo<sup>28,29</sup>. The current pulse sequence operates in identical fashion on the triplet spin manifold (which is also spin-1), except that the degeneracy of the triplet-triplet transitions is not broken by quadrupolar couplings, but by the small chemical shift difference between the coupled nuclei. We therefore use the term triplet echo (TE). As in the case of the quadrupolar echo, the relative phase of the central  $90^\circ$  pulse and the transverse magnetization is important. In the different regime of a large chemical shift difference (the weak-coupling limit), the same pulse sequence (omitting the initial and final  $90^\circ$  pulses) refocuses homonuclear J-couplings. In this context, the sequence is known as the perfect echo<sup>30,31</sup>.

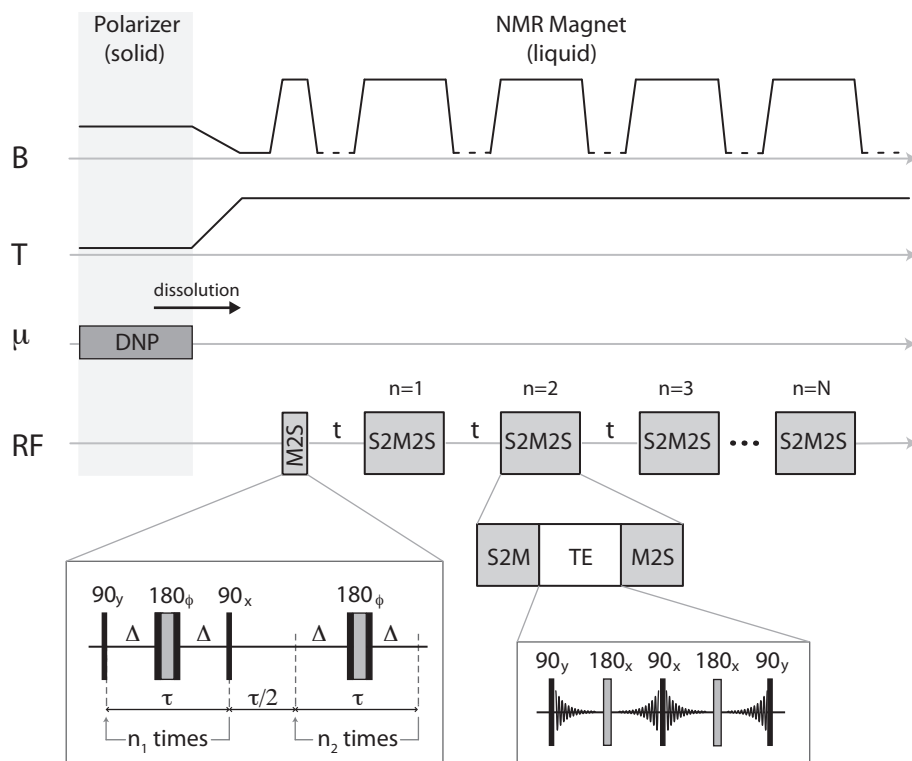


**Figure 2.** Pulse sequence used to demonstrate recycled observation of the same batch of highly polarized singlet order. Trace B shows the trajectory of magnetic field as the sample is transported from the polarizer to the high-field magnet and through a region of low field; trace T shows the temperature changes from  $\sim 1.4$  K to room temperature across the experiment; trace  $\mu$  shows the microwave irradiation applied during dissolution-DNP; trace RF shows the radiofrequency pulses applied at the nuclear resonance frequency in high magnetic field. Expansions of M2S and TE blocks are shown. The S2M pulse sequence is equal to the M2S sequence applied in reverse-chronological order. The time axis is not to scale. The field cycling between S2M2S blocks is necessary for samples with significant isotropic shift differences but may be omitted if the isotropic shift difference is small enough.

The S2M-TE-M2S combination is abbreviated here as S2M2S, and allows nuclear singlet order to be converted temporarily into transverse magnetization, where it gives rise to an observable NMR signal. The NMR signal may be observed during all four interpulse intervals of the TE pulse sequence, after which singlet order is regenerated by the final M2S pulse sequence. Repeated S2M2S blocks may therefore be used for multiple observations of the same batch of long-lived singlet order, with only modest losses on each pass, associated with relaxation losses during the triplet echoes, and pulse imperfections.

The experiment shown in Figure 2 runs as follows: (1) The nuclear spin polarization of the sample is enhanced by dissolution-DNP; (2) an M2S pulse sequence is applied in order to convert the enhanced longitudinal magnetization into singlet order; (3) the sample is transported to a region of low magnetic field where magnetic equivalence is imposed

through minimization of the chemical shift interaction; (4) the sample is kept in the low field for a time interval  $t$ ; (5) an S2M2S pulse sequence is applied, using a triplet echo of duration  $\tau = 408$  ms. The NMR signal is observed during the interpulse delays of the TE sequence; (6) Steps 4 and 5 are repeated  $N$  times until the singlet polarization has decayed.

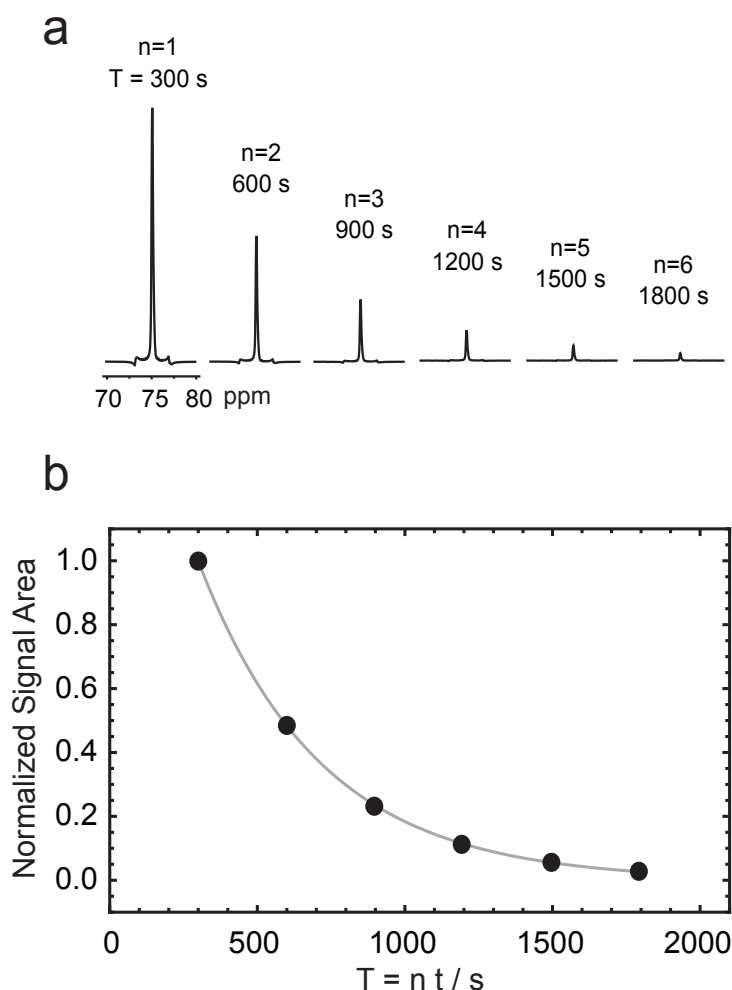


**Figure 3.** Decay of the hyperpolarized- $^{13}\text{C}$  NMR signal stored as singlet order on Sample 1. (a) Spectra obtained by Fourier-transforming the first FID acquired during each triplet echo. (b) Signal areas of the spectra in (a) plotted as a function of the low field storage total interval  $T = nt$ , where the interval between S2M2S blocks is  $t = 300$  s, and  $n$  takes values 1,2..6. The solid grey line is the best fit to an exponential decay. All NMR signals are acquired at 9.4 T, while the storage of singlet order between pulse sequences is at a field of  $\sim 20$  mT.

In the experiment described here, the sample is removed from the magnet between S2M2S blocks, in order to suppress singlet-triplet transitions caused by the isotropic chemical shift difference. This is necessary for sample 1, which has a relatively large chemical shift difference, although field cycling is not necessary for samples where the spin pair is closer to perfect magnetic equivalence.

The series of spectra obtained on sample 1 is shown in Figure 3a. These spectra are Fourier transforms of the first free-induction decay observed during each TE echo sequence; The signal-to-noise ratio obtained after the first passage through step 5 ( $n=1$ ) is  $\sim 2350$  while the signal-to-noise ratio for the spectrum obtained at the 6-th passage ( $n=6$ ) is  $\sim 65$ . The filled circles in Fig. 3b represent the area underneath the peak at 75 ppm. The decay curve is a good fit to a single exponential decay with a time constant,  $410 \pm 2$  s. The decay time constant is roughly half the singlet time constant of  $T_S = 800 \pm 43$  s measured on the same sample but thermally polarized at 298K and 9.4T, and without recycled observation of the same singlet order. The discrepancy is attributed to pulse imperfections and relaxation during the S2M2S sequences contribute to a  $\sim 10\%$  loss of singlet order on each pass. Some decay of singlet order may also be caused by the radical species used in

the DNP process (see Sec. 2.2 and Supporting Information); however, paramagnetic relaxation by radicals is unlikely to be serious in the current case, since spontaneous precipitation of the radical in CD<sub>3</sub>CN was observed (although not quantitatively characterized) during the dissolution step.

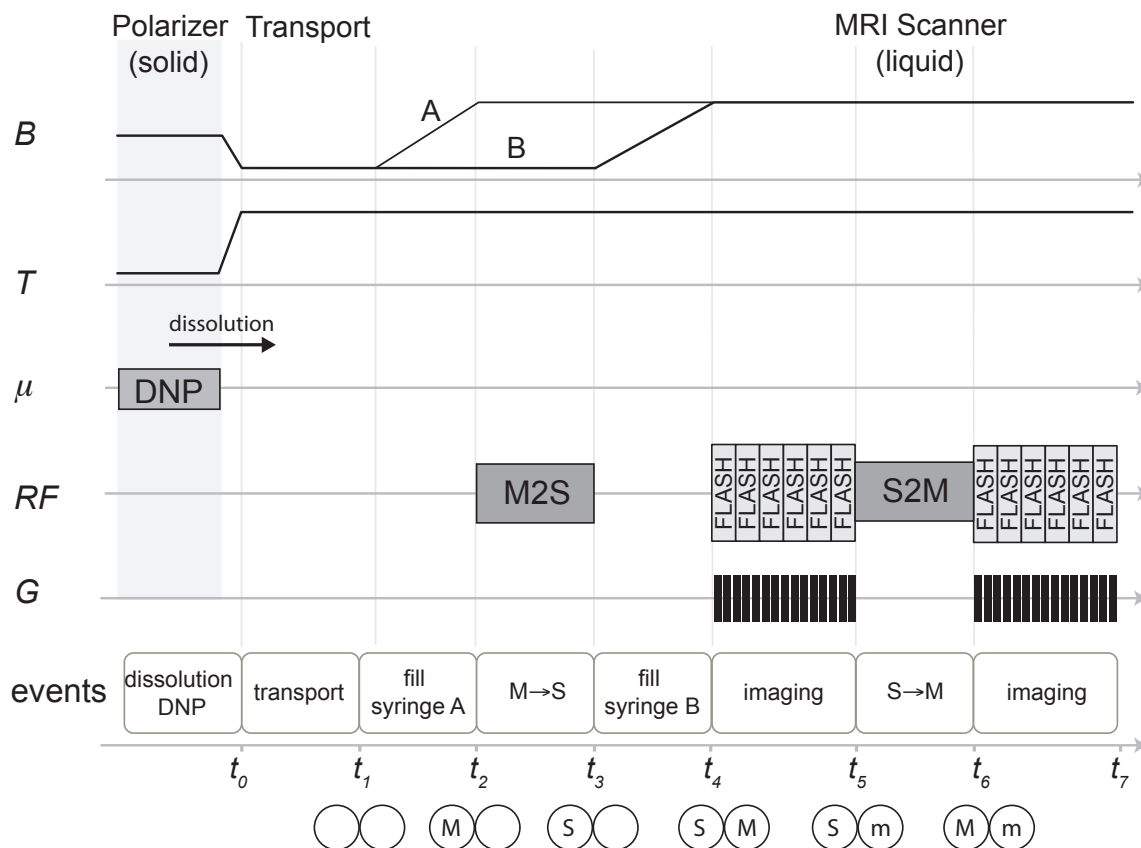


**Figure 4.** Timing sequence of the singlet MRI experiment. Trace *B* shows the magnetic fields to which samples ending up in the two syringes are exposed; the sample is divided at time point  $t_1$  and loaded into syringe A before syringe B; trace *T* shows the temperature changes from  $\sim 1.4$  K to room temperature; trace  $\mu$  shows the microwave irradiation applied during dissolution-DNP; trace *RF* shows the radiofrequency pulses applied at the resonant frequency of the nuclei in the MRI magnet. Trace *G* sketches the pulsed field gradients during the imaging sequences. The time points are indicated. The polarization states in the two syringes are shown below the diagram: "M" indicates a sample possessing highly polarized magnetization; "S" indicates highly polarized singlet order; "m" indicates residual magnetization.

We point out that the first M2S sequence cannot convert all of the magnetization into singlet order, since the eigenvalues of the density operator are preserved upon this unitary transformation<sup>32,33</sup> (see Supplementary Information). The fundamental conversion limit for this transformation is  $\sqrt{2/3} \sim 81.6\%$ , so even in an ideal experiment where there is no signal loss due to relaxation or pulse imperfections, there is  $\sim 18\%$  loss of magnetization upon the first conversion into singlet order.

The results shown in Figure 3 show that it is possible to store hyperpolarization as singlet order and observe it repeatedly, with full intensity, over a time interval of many tens of minutes. Note that nuclear spin magnetization would already have decayed to an insignificant level before even the first observation point in Figure 3.

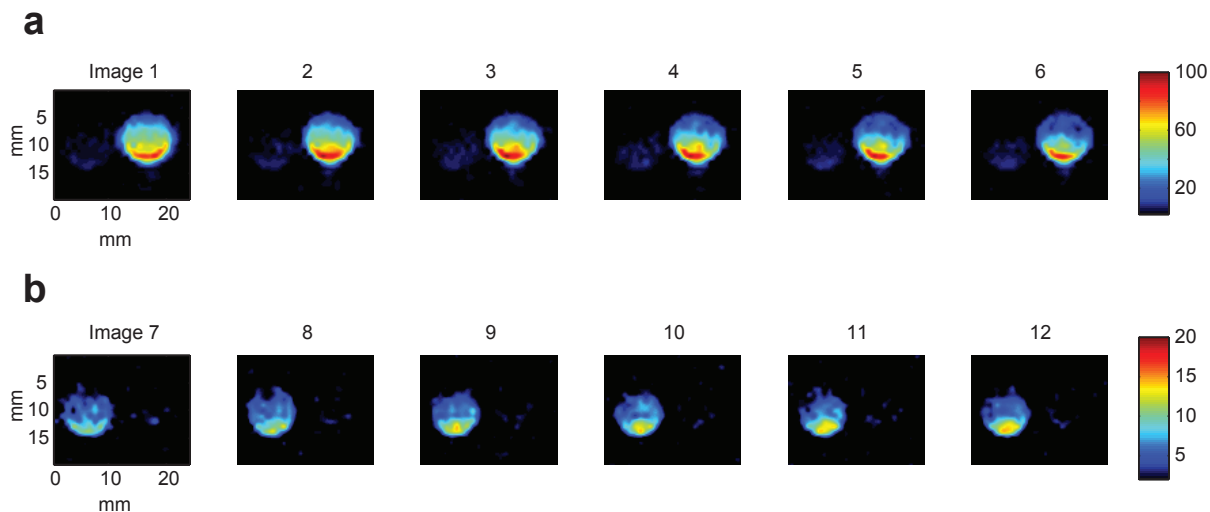


**Figure 5.** The series of  $^{13}\text{C}$  MR images resulting from the experiment in Fig. 4, using sample 2 in Fig.1. (a) images acquired between time points  $t_4$  and  $t_5$ , and (b) between time points  $t_6$  and  $t_7$ . Syringe A appears on the left, and syringe B on the right. During acquisition of the images in row (a), syringe A contains highly polarized singlet order, while syringe B contains highly polarized magnetization. Before acquisition of the images in row (b), the singlet order in syringe A is converted into magnetization by a S2M pulse sequence. These results show that the singlet order survives a FLASH-MRI pulse sequence, albeit with loss of intensity.

### 3.2 Storage and retrieval of hyperpolarized spin order in MRI

In order to demonstrate the possibilities of singlet storage in MRI, we performed a simple *in vitro* MRI experiment on a small-animal scanner. The experiment exploits the high selectivity of the M2S and S2M pulse sequences, which only convert magnetization into singlet order, and vice versa, if the pulse sequence timings closely match the spin-spin couplings in the system. This selectivity makes it possible to conduct an entire MRI experiment on hyperpolarized magnetization without disturbing the amount of hyperpolarized singlet order created in the same object.

A phantom was constructed of two plastic syringes (A and B) taped side-by-side and placed on top of a surface coil used for detection (Fig. S3, Supplementary Information). The surface coil and phantom were placed inside a volume transmit coil in the bore of a 4.7 T horizontal MRI scanner. The syringes were connected to two plastic tubes, which were filled with 0.2 mL of deuterated methanol. The pistons of the syringes were initially fully inserted. Each syringe could be filled from outside the magnet by pushing a sample through its connecting tube using a third syringe.

The time sequence of the MRI experiment is shown in Fig. 4, and runs as follows: (1) Sample 2's nuclear spin polarization (Figure 1) is enhanced by dissolution-DNP. 2 mL of the polarized sample are collected in a transport syringe placed next to the polarizer in a magnetic field of  $\sim 5$  G; (2) within  $\sim 5$  s, the transport syringe containing the sample is carried over to the MRI scanner and half of its content is transferred to syringe A by injection through one of the two plastic tubes; the other half is left in the stray field of the scanner; (3) a M2S sequence is applied to convert the magnetization in syringe A into singlet order; (4) syringe B is filled with the other half of the original highly polarized sample; (5) a FLASH<sup>54</sup> MRI pulse sequence is used to acquire a series of six consecutive  $^{13}\text{C}$  images of the phantom (pulse sequence and parameters described in the Supplementary Information); (6) a S2M sequence is applied to convert the content of syringe A from singlet order into magnetization. (7) A second series of six consecutive  $^{13}\text{C}$  images is acquired using the same methodology as in step 5.

Steps 1-4 prepare a phantom loaded with hyperpolarized singlet order in one part (in this case, in syringe A), while a different part of the same phantom contains hyperpolarized magnetization (in this case, in syringe B). The imaging sequence generates signals from the hyperpolarized magnetization (in syringe B), while hyperpolarized singlet order (in syringe A) is left substantially undisturbed by the imaging procedure. At the end of the imaging sequence, the singlet order in syringe A is converted into magnetization and imaged. The results in Figure 5 show that this procedure works, in principle. The weaker intensity in (b) compared to (a) is attributed to pulse imperfections and relaxation losses.

The results in Figure 5 illustrate a form of duplexing. Highly polarized spin order is simultaneously present in two different forms (magnetization and singlet order) in the same object. Magnetization may first be imaged, while the singlet order remains, to be used for imaging at a later time.

## 4. Conclusions

The two experiments described here demonstrate (1) the long time storage of the polarization enhancement obtained by dissolution-DNP using a long-lived singlet state involving two  $^{13}\text{C}$  nuclei; (2) a protocol for repeated observation of the singlet order with only a minor loss of intensity upon each observation cycle; (3) the possibility of conducting a MRI experiment on highly polarized magnetization while highly polarized singlet order remains relatively unperturbed.

In these experiments, singlet order in the near-equivalent  $^{13}\text{C}_2$  spin system resembles a "spin bank" or "resealable container" in which polarization is deposited for safe-keeping.

The analogy with a "bank" or "resealable container" may be pushed further: The M2S and S2M pulse sequences are narrowband with respect to the J coupling of the  $^{13}\text{C}_2$  spin pair and therefore resemble "keys" for the "deposit" (M2S) and "retrieval" (S2M) of singlet spin order. The "container" is not completely leak-proof - the deposited spin order decays in time (inflation). Even the physical limits associated with the unitary transformation of magnetization into singlet order, and *vice versa*, resemble the deposit and withdrawal regulations applying to certain types of bank account. Unfortunately, there appears to be no physical analogy for interest. However, banks rarely give an interest rate higher than inflation (unfortunately), which establishes the analogy. Hyperpolarization has another educating analogy to the real world of finance: Once spent, it does not come back.

The use of singlet states in metabolic studies is limited to the natural occurrence of endogenous suitable molecules. Highly polarized singlet states in  $^{13}\text{C}_2$ -pyruvate for *in-vivo* metabolic preclinical studies allow more time for handling the substrate prior to injection and reducing the losses during circulation in the blood stream (as recently observed in ongoing experiments). Furthermore, the design of biocompatible molecules that support long-lived states (ongoing in our laboratory) allows the distribution/concentration of highly polarized molecular probes in the body. Properly engineered molecules would preserve their polarization while travelling in the body therefore opening access to more remote organs. Both these important applications are currently out of reach in MRI because of the short life of longitudinal polarization. In the design of such molecules, other relaxation contributions such as solvent induced relaxation<sup>35</sup>, for example, may need attention and the singlet spin pair may require to be embedded in the core of the molecule, far from direct contact with the solvent.

## ASSOCIATED CONTENT

**Supporting Information Available.** Synthetic Routes; Dissolution-DNP procedure; NMR pulse sequence details; MRI Hardware and pulse sequence details; Singlet and triplet states and singlet order; Unitary limits on magnetization-to-singlet transformations. This information is available free of charge via the Internet at <http://pubs.acs.org>.

## AUTHOR INFORMATION

### Corresponding Author

\* [g.pileio@soton.ac.uk](mailto:g.pileio@soton.ac.uk)

### Present Addresses

† Institute for Molecules and Materials, Radboud University Nijmegen, Heyendaalseweg 135, 6525 AJ Nijmegen, The Netherlands.

### Notes

The authors declare no competing financial interest.

## ACKNOWLEDGMENT

This research is supported by EPSRC (UK) and ERC.

## REFERENCES

- (1) Overhauser, A. *Phys. Rev.* **1953**, 92, 411–415.
- (2) Boer, W. J. *Low Temp. Phys.* **1976**, 22, 185–212.
- (3) Abragam, A.; Goldman, M. *Rep. Prog. Phys.* **1978**, 41, 395–467.
- (4) Ardenkjaer-Larsen, J. H.; Fridlund, B.; Gram, A.; Hansson, G.; Hansson, L.; Lerche, M. H.; Servin, R.; Thaning, M.; Golman, K. *Proc. Natl. Acad. Sci. U.S.A.* **2003**, 100, 10158–63.

- (5) Bowers, C. R.; Weitekamp, D. P. *J. Am. Chem. Soc.* **1987**, 109, 5541–5542.
- (6) Levitt, M. H. *Encyclopedia of Magnetic Resonance*; Harris, R. K.; Wasylishen, R. E., Eds.; John Wiley & Sons, Ltd: Chichester, UK, 2010.
- (7) Levitt, M. H. *Ann. Rev. Phys. Chem.* **2012**, 63, 89–105.
- (8) Carravetta, M.; Levitt, M. H. *J. Chem. Phys.* **2005**, 122, 214505.
- (9) Carravetta, M.; Johannessen, O.; Levitt, M. *Phys. Rev. Lett.* **2004**, 92, 1–4.
- (10) Pileio, G.; Levitt, M. H. *J. Chem. Phys.* **2009**, 130, 214501.
- (11) Pileio, G. *Prog. Nucl. Magn. Reson. Spect.* **2010**, 56, 217–31.
- (12) Tayler, M. C. D.; Levitt, M. H. *Phys. Chem. Chem. Phys.* **2011**, 13, 9128–30.
- (13) Pileio, G.; Carravetta, M.; Hughes, E.; Levitt, M. H. *J. Am. Chem. Soc.* **2008**, 130, 12582–3.
- (14) Ghosh, R. K.; Kadlecsek, S. J.; Ardenkjaer-Larsen, J. H.; Pullinger, B. M.; Pileio, G.; Levitt, M. H.; Kuzma, N. N.; Rizi, R. R. *Magn. Reson. Med.* **2011**, 66, 1177–80.
- (15) Pileio, G.; Hill-Cousins, J. T.; Mitchell, S.; Kuprov, I.; Brown, L. J.; Brown, R. C. D.; Levitt, M. H. *J. Am. Chem. Soc.* **2012**, 134, 17494–7.
- (16) Franzoni, M. B.; Buljubasich, L.; Spiess, H. W.; Münnemann, K. *J. Am. Chem. Soc.* **2012**, 134, 10393–6.
- (17) Laustsen, C.; Pileio, G.; Tayler, M. C. D.; Brown, L. J.; Brown, R. C. D.; Levitt, M. H.; Ardenkjaer-Larsen, J. H. *Magn. Reson. Med.* **2012**, 68, 1262–5.
- (18) Warren, W. S.; Jenista, E.; Branca, R. T.; Chen, X. *Science* **2009**, 323, 1711–4.
- (19) Vasos, P. R.; Comment, A.; Sarkar, R.; Ahuja, P.; Jannin, S.; Ansermet, J.-P.; Konter, J. A.; Hautle, P.; van den Brandt, B.; Bodenhausen, G. *Proc. Natl. Acad. Sci. U.S.A.* **2009**, 106, 18469–73.
- (20) Bornet, A.; Jannin, S.; Bodenhausen, G. *Chem. Phys. Lett.* **2011**, 512, 151–154.
- (21) Golman, K.; Zandt, R. I.; Lerche, M.; Pehrson, R.; Ardenkjaer-Larsen, J. H. *Cancer Res* **2006**, 66, 10855–10860.
- (22) Golman, K.; in 't Zandt, R.; Thaning, M. *Proc. Natl. Acad. Sci. U.S.A.* **2006**, 103, 11270–5.
- (23) Day, S. E.; Kettunen, M. I.; Gallagher, F. a; Hu, D.-E.; Lerche, M.; Wolber, J.; Golman, K.; Ardenkjaer-Larsen, J. H.; Brindle, K. M. *Nature medicine* **2007**, 13, 1382–7.
- (24) Tayler, M. C. D.; Marco-Rius, I.; Kettunen, M. I.; Brindle, K. M.; Levitt, M. H.; Pileio, G. *J. Am. Chem. Soc.* **2012**, 134, 7668–71.
- (25) Pileio, G.; Carravetta, M.; Levitt, M. H. *Proc. Natl. Acad. Sci. U.S.A.* **2010**, 107, 17135–9.
- (26) Tayler, M. C. D.; Levitt, M. H. *Phys. Chem. Chem. Phys.* **2011**, 13, 5556–60.
- (27) Feng, Y.; Davis, R. M.; Warren, W. S. *Nature Physics* **2012**, 8, 1–4.
- (28) Solomon, I. *Phys. Rev.* **1958**, 110, 61–65.
- (29) Weisman, I.; Bennett, L. *Phys. Rev.* **1969**, 181, 1341–1350.
- (30) Aguilar, J. A.; Nilsson, M.; Bodenhausen, G.; Morris, G. A. *Chem. Comm.* **2012**, 48, 811–3.



- (31) Takegoshi, K.; Ogura, K.; Hikichi, K. *J. Magn. Reson. (1969)* **1989**, 84, 611–615.
- (32) Levitt, M. H. *J. Magn. Reson. (1969)* **1992**, 99, 1–17.
- (33) Sørensen, O. W. *J. Magn. Reson. (1969)* **1990**, 86, 435–440.
- (34) Frahm, J.; Haase, A.; Matthaei, D. *Magn. Reson. Med.* **1986**, 3, 321–327.
- (35) Pileio, G. *J. Chem. Phys.* **2011**, 134, 214505.

